multaneously. The real-time measurements are complemented by post-growth AFM and XRR measurements.

The out-of-plane thickness dependent structure of the thin films, including the coverage of molecular layers and out-of-plane lattice constant, is probed using XRR measurements at the anti-Bragg condition. We apply a growth model first proposed by Trofimov et al. [5] in combination with kinematical scattering theory [6] to simulate the XRR data. Additionally, we need to implement thickness dependent lattice constant to fully describe the experimental observations. The detailed analysis reveals the layer-by-layer growth mode in the first two molecular layers and an onset of the film roughening from the third monolayer onwards. Additionally, we observe change of the out-of-plane lattice spacing and concomitant change of molecular tilt during the growth of the $2^{nd} - 4^{th}$ monolayer.

The in-plane structure of the thin films is probed using GISAXS measurements (see Fig. 1), which allow for determining thickness dependent distance of molecular islands and their size. We use the temperature dependence of the island size to determine effective activation energy of island nucleation in different layers. The effective energy in the 2^{nd} layer is smaller than that in the 1^{st} layer. The difference in activation energies explains the fact that islands grow smaller in the 1^{st} layer than in the 2^{nd} layer as observed using GISAXS and also in AFM post-growth images.

In conclusion, combined *in situ* real-time GISAXS and XRR measurements bring insight into the growth of the first few monolayers of DIP thin films. In particular, we are able to capture the transition from layer-by-layer growth to the thin film roughening and the change of lattice parameters during the growth and to identify difference in activation energies for the first two molecular layers.

1. Physics of Organic Semiconductors, edited by W. Brütting (Wiley-VCH, Weinheim, 2005).
2. S. Kowarik, A. Gerlach, S. Sellner, F. Schreiber, L. Cavalcanti, and O. Konovalov, *Phys. Rev. Lett*., **96**, (2006), 125504.
3. R. Banerjee, J. Novák, C. Frank, C. Lorch, A. Hinderhofer, A. Gerlach, and F. Schreiber, *Phys. Rev. Lett*., **110**, (2013), 185506.
4. K. A. Ritley, B. Krause, F. Schreiber, and H. Dosch, *Rev. Sci. Instrum*., **72**, (2001), 1453.
5. V. I. Trofimov and V. G. Mokerov, *Thin Solid Films*, **428**, (2003), 66.
6. S. Kowarik, A. Gerlach, M. W. A. Skoda, S. Sellner, and F. Schreiber, *Europ. Phys. J.- Special Topics*, **167**, (2009), 11.

We gratefully acknowledge the financial support of the DFG. We also acknowledge J. Krug (University Köln) and S. Bommel (Humboldt University Berlin) for helpful discussions and F. Anger (University Tübingen) for help during experiments.

Session III, Wednesday - morning, September 11

L9

SMALL-ANGLE NEUTRON SCATTERING CONTRIBUTION TO DEVELOPMENT OF SOME NOVEL MATERIALS

P. Strunz[1], D. Mukherji[2], M. Petrenec[3], R. Gilles[4], G. Schumacher[5], G. Pigozzi[6], U. Keiderling[5], T. Geue[7], U. Gasser[7], J. Šaroun[1] and J. Rösler[2]

[1]Nuclear Physics Institute ASCR, CZ-25068 Řež near Prague, Czech Republic
[2]TU Braunschweig, Institut für Werkstoffe, Langer Kamp 8, 38106 Braunschweig, Germany,
[3]IPM Brno, Czech Republic and TESCAN, a.s., Czech Republic
[4]TU München, Forschungsneutronenquelle Heinz Maier-Leibnitz (FRM II), Lichtenbergstraße 1, 85747 Garching, Germany
[5]Helmholtz Centre Berlin for Materials and Energy GmbH, Glienickerstr. 100, D-14109 Berlin, Germany
[6]Laboratory for Corrosion and Materials Integrity, EMPA Duebendorf, Switzerland
[7]Laboratory for Neutron Scattering, Paul Scherrer Institute, CH-5232 Villigen, Switzerland
strunz@ujf.cas.cz

Basic advantages and disadvantages of neutron radiation and its interaction with matter - with respect to materials research by means of neutron diffraction - are listed. The areas of Small-Angle Neutron Scattering (SANS) [1] application in materials science are discussed.

Several examples of the use of SANS to microstructural characterization of technologically important metallic materials are shown. First, a contribution of in-situ SANS to a solution of an open question in INCONEL polycrystalline superalloy load characteristics is reported. Secondly, evolution of ′-precipitate morphology in pre-deformed single-crystal Ni-base superalloy at elevated temperatures is determined. Afterwards, characterization of a porous membrane prepared by selective phase dissolution process from the single-crystal Ni superalloy is presented. Further, SANS characterization of Ni_3Si-type nanoparticles dispersed in a mixture of H_2O/D_2O using the contrast variation method is shown. Finally, the investigation of a model system (Al-Pb) for testing liquid-phase dispersion strengthening is discussed.

Precipitate microstructure evolution in exposed IN738LC superalloy

Nickel-base superalloy IN738LC has been studied after low-cycle fatigue by SANS [1,2]. Samples subjected to high-temperature low-cycle fatigue [4] were annealed at various temperatures to change the size and the distribution of precipitates. Ex- and in-situ SANS and high resolution TEM studies were performed. It was found by SANS that additional precipitates are produced either during slow cooling from high temperatures or after reheating above 570°C (Fig. 1). Their size and distribution were evaluated. The precipitates arise regardless the application of the mechanical load. Nevertheless, these small precipitates influence low-cycle fatigue resistance. From the SANS data, it can be also deduced that the equilibrium volume fraction of ′-precipitates at temperatures from room temperature to 825 °C is significantly higher than previously reported 45%. The kinetics of formation of small and medium-size ′ precipitates at 700 and 800 °C was determined as well.

Morphology changes of ă' precipitates in pre-deformed single-crystal Ni-base superalloy

Exposure of a superalloy to an external load results in anisotropic coarsening of the ' precipitates (rafting). ă' rafting can also occur as a result of purely thermal treatment, without the simultaneous presence of an external load, if the specimen has been pre-deformed at relatively low temperature. The evolution of ' morphology in pre-deformed specimens of SCA425 Ni-base superalloy was examined [5]. SANS data provide indication of rafting during the subsequent heating after severe compressive pre-straining (2%).

Pore structure characterization in nanoporous membrane

Using a selective phase dissolution technique, nano-porous membrane can be produced from simple two-phase metallic alloys. It contains through-thickness elongated channel-like pores of only a few hundred nanometer width and has a number of prospective applications. Knowledge of microstructural parameters is essential for membrane optimization. Non-destructive characterization of the pore microstructure was carried out by SANS technique [6]. The combined results from pinhole (Fig. 2) and double-crystal facilities enabled to determine microstructural parameters of the nanoporous membrane (pore-to-pore distance, raft thickness, pore volume fraction, specific interface). The contrast variation using D_2O and H_2O helped to conclude on scattering length density of both ′ pore walls as well as the original -phase matrix.

Characterization of core-shell nanoparticles

The Ni_3Si-type nanoparticles dispersed in a mixture of H_2O/D_2O were characterized by SANS using the contrast variation method. The nanoparticles were produced by extracting precipitates from a bulk Ni-13.3Si-2Al (at.%) alloy using electrochemical phase separation technique and were pre-characterized by X-ray diffraction and transmission electron microscopy. The existence of a core-shell structure in the nanoparticles with a Ni_3Si*(*Al*)* core and amorphous SiO_x shell was confirmed by the SANS measurements [7]. By comparing the precipitate morphology in the Ni-Si-Al alloy with the extracted nanoparticles, it was clearly established that the size of precipitates is unaffected by the extraction process and that the amorphous shell forms on top of the particle core.

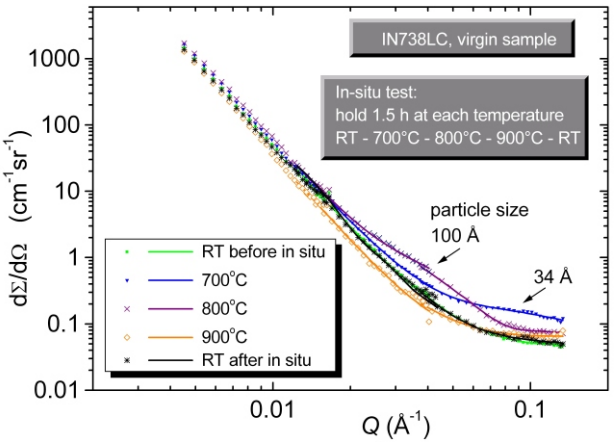

Figure 1. In-situ SANS for non-cycled sample: in-situ heating RT-700-800-900°C-RT (hold at each temperature during the in-situ SANS was always 1.5 hour).

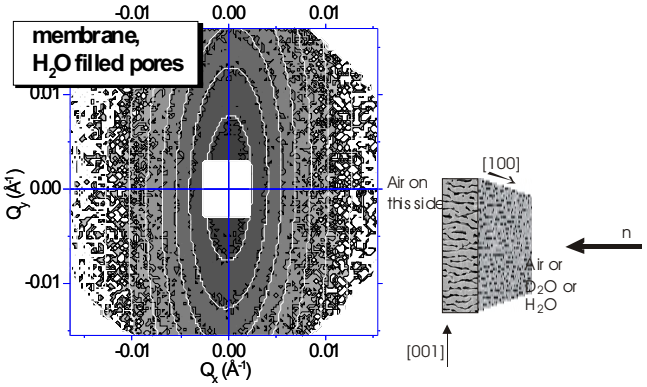

Figure 2. 2D cross-section d /d (Q_x,Q_y) is shown (left) for H_2O filled pores of the porous membrane (scheme shown on right). The grey scale map shows measured 2D data and the white equi-intensity lines depict the fitted curves. V4 pinhole SANS, BENSC, HZ Berlin.

Metal-matrix composite containing liquid-phase dispersion

Al-Pb binary system is a suitable model system for testing liquid phase dispersion strengthening in bulk materials for structural applications. Liquid Pb islands can be finely dispersed in still solid Al matrix due to the substantial difference of melting points. The Al-Pb system prepared by means of Equal Channel Angular Pressing (ECAP) process was investigated by Small-Angle Neutron Scattering technique (SANS) which enables in-situ measurement of size and morphology parameters of Pb inclusions at elevated temperatures. It was observed that the lead particles were elongated roughly in the direction of ECAP [8]. During the subsequent in-situ thermal cycle RT-400°C-RT, the elongated Pb particles transformed to nearly spherical shape. The change of scattering contrast during melting of Pb mapped the transform of the confined lead particles to the

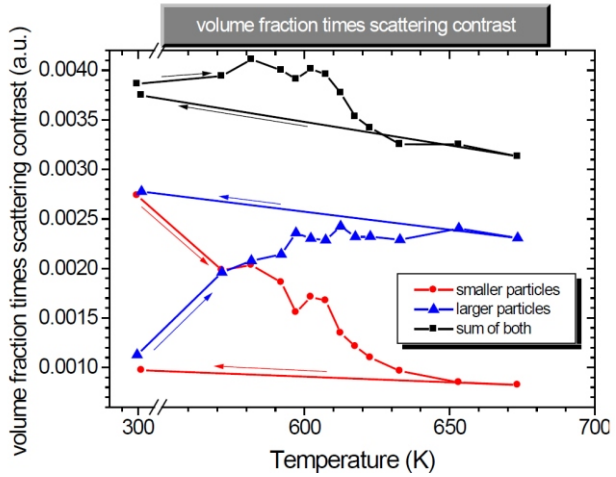

Figure 3. The temperature dependence of volume fraction times scattering contrast of confined Pb particles in the Al-4%Pb ECAP sample during the thermal cycle.

liquid phase. The center of the transition region is around 342°C (615K) for both the as-cast and the ECAP deformed samples, which is a significant shift with respect to the free Pb melting point 327°C (600K). For the ECAP sample, the transition is not sharp, indicating a broad size distribution of lead particles (Fig. 3).

References

1. G. Kostorz, in: Neutron Scattering (Treatise on materials science and technology), G. Kostorz (Eds.), Academic Press, New York, 1979, pp.227-289.
2. P. Strunz, M. Petrenec, U. Gasser, in Proceedings of the 15th International Small-Angle Scattering Conference, Sydney, Australia, 18-23 November 2012. D. McGillivary, J. Trewhella, E.P. Gilbert, T.L. Hanley (Eds.), Australian Nuclear Science and Technology Organisation, ISBN 1 921268 15 8, paperlessevent.com.au/SAS2012.zip.
3. P. Strunz, M. Petrenec, U. Gasser, J. Tobiáš, J. Polák and J. Šaroun, submitted to Journal of Alloys and Compounds, 2013.
4. M. Petrenec, J. Tobiáš, J. Polák, M. Šmíd, A. Chlupová, R. Petráš, in Proc. of XVI International Colloquium Mechanical Fatigue of Metals, J. Polák, T. Kruml, J. Man (Eds.), ISBN 978-80-87434-05-5, ÚFM AVČR, Brno, 2012, pp. 245-250.
5. P. Strunz, G. Schumacher, H. Klingelhöffer, A. Wiedenmann, J. Šaroun, U. Keiderling, J. Appl. Cryst. 44 (2011) 935–944.
6. P. Strunz, D. Mukherji, J. Šaroun, U. Keiderling, J. Rösler, Journal of Physics: Conference Series 247 (2010), 012023, doi:10.1088/1742-6596/247/1/012023.
7. P. Strunz, D. Mukherji, G. Pigozzi, R. Gilles, T. Geue, K. Pranzas, Appl. Phys. A 88 (2007) 277-284.
8. P. Strunz, D. Mukherji, R. Gilles, T. Geue and J. Rösler, J. Phys.: Conf. Ser. 340 (2012) 012098, doi: http://iopscience.iop.org/1742-6596/340/1/012098.

Acknowledgements

The support by GACR project No. P204/11/1453 is gratefully acknowledged. The authors thank SINQ (PSI Villigen, Switzerland), NPL (CANAM), NPI Řež, Czech Republic) and BENSC (HZB Berlin, Germany) for providing beamtime and support for the SANS measurements. Infrastructure projects support (NMI3-II EC project No. 283883 and CZ MSMT project No. LM2011019) are gratefully acknowledged as well.

L10

UTILIZATION OF SANS FOR INVESTIGATION OF MAGNETIC STRUCTURES AND DYNAMICS

V. Ryukhtin

Nuclear Physics Institute ASCR, Řež near Prague, Czech Republic
ryukhtin@ujf.cas.cz

There are plenty interesting examples of magnetic structures studied by small-angle neutron scattering (SANS). Here we would like to present several successful topics of the SANS usage. For example, the very first experimental observation of magnetic flux line lattices (FLL) - magnetic vortexes in type II superconductors - have been done using SANS. General approach as well as practical details of FLL measurements will be demonstrated. Other example is ferrofluids based on magnetic nanoparticles. SANS can be used for not just for structural characterizations but also for studying of their dynamics using stroboscopic and TISANE options.

L11

SANS EXPERIMENT ON SUPERPLASTIC CERAMICS

V. Ryukhtin

Nuclear Physics Institute ASCR, Řež near Prague, Czech Republic
ryukhtin@ujf.cas.cz

Superplastic (SP) deformation of fine grained materials (FGM) is accompanied by creation of cavities and cracks. Cavitation processes describe quantitatively driving mechanisms such as grain boundary sliding (GBS). Small angle neutron scattering (SANS) can be effectively used for characterization of cavitaion in yittria stabilized zirconia (3Y-TZP) undergoing SP deformation. We would like to present results of pin-hole and double-crystal SANS measurements with treatment and interpretation demonstrating effective description of bulk cavitation. Treatment and fitting of these results will be explained in the followed presentations.

L12

X-RAY STUDY OF NUCLEATION AND GROWTH OF PRECIPITATES OF -PHASE IN Ti ALLOYS

J. Šmilauerová[1], P. Harcuba[1], J. Stráský[1], M. Janeček[1], J. Pospíšil[2], Z. Matěj[2], J. Ilavský[3] and V. Holý[2]

[1]Department of Material Physics, Faculty of Mathematics and Physics, Charles University in Prague, Ke Karlovu 5, 121 16 Praha, Czech Republic
[2]Department of Condensed Matter Physics, Faculty of Mathematics and Physics, Charles University in Prague, Ke Karlovu 5, 121 16 Praha, Czech Republic[3] Argonne National Laboratory, IL, USA
holy@mag.mff.cuni.cz

Metastable titanium alloys are of great interest to the automotive, aerospace and biomedical industry due to their outstanding mechanical properties. Depending on the stability of phase in metastable titanium alloy, several metastable phases can form. Probably the most important and most frequently studied metastable phase is the phase formed during quenching by a diffusionless displacive transformation. We have studied this process by x-ray diffraction (XRD) and small-angle x-ray scattering (SAXS) performed on single crystals of titanium alloy (Ti-6.8Mo-4.5Fe-1.5Al in wt.%). XRD experiments have been carried out on a standard x-ray laboratory source (CuK , 1.6 kW) using two geometries. In the low-resolution setup (polycapillary optics, parallel-plate collimator and secondary graphite monochromator) we measured pole figures in diffraction maxima of both and phases before and after ageing annealing at 300 °C. From the measurement a distinct topotaxy relation between the and lattices follows. Further, we used a middle-resolution setup (parabolic x-ray mirror on the primary side) for the measurement of coplanar reciprocal space maps around and diffraction maxima. From the maps we determined the size of the particles in the host lattice, their lattice parameters and local lattice deformation around the particles. The results of the diffraction studies are in press [1].

SAXS measurements have been carried out at APS Argonne, USA, using the photon energy of 20 keV. The experimental data clearly indicate that the -particles are self-organized; they create a disordered cubic lattice. From the data we determine the mean particle distance and the degree of ordering as functions of the ageing time. We developed a numerical model based on a Monte-Carlo simulation of the nucleation and growth of particles that qualitatively explains the measured data.

1. J. Šmilauerová, P. Harcuba, J. Pospíšil, Z. Matej and V. Holý, Acta Mater. (in press).

L13

SCANNING X-RAY SUBMICRON DIFFRACTION ON 3D HETEROEPITAXIAL MICROCRYSTALS

M. Meduňa[1], C.V. Falub[2], D. Chrastina[3], F. Isa[3], A. Marzegalli[4], T. Kreiliger[2], A. G. Taboada[2], G. Isella[3], L. Miglio[4], H. von Känel[2]

[1]Department of Condensed Matter Physics & CEITEC, Masaryk University, Kotlářská 2, 61137 Brno, Czech Republic
[2]Laboratory for Solid State Physics, ETH-Zürich, Schafmattstrasse 16, 8093 Zürich, Switzerland
[3]L-NESS, Department of Physics, Politecnico di Milano, via Anzani 42, 22100 Como, Italy
[4]L-NESS, Department of Materials Science, Universita di Milano-Bicocca, via Cozzi 53, 20126 Milano, Italy
mjme@physics.muni.cz

Monolithic integration of other semiconductor materials onto silicon substrates is expected to extend Si-based technology towards new optical and electrical functionalities inaccessible by the mere dimensional scaling predicted by Moore's Law. Unless wafer bonding techniques are used, such integration of dissimilar materials necessarily involves hetero-epitaxial growth. However, the growth of epitaxial layers on a single crystal substrate usually results in undesired defect formation above a certain critical thickness, if the corresponding crystal lattices exhibit a poor match of lattice parameters or thermal expansion coefficients.

Recent achievements demonstrate that extremely thick Ge-layers with exceptional crystalline quality can be monolithically integrated onto a Si CMOS platform despite the large lattice and thermal mismatches. Dislocations, layer cracking and wafer bowing could all be eliminated by a novel mask-less deposition process wherein high-quality Ge towers are epitaxially grown by LEPECVD technique on micron size structures with high aspect ratios machined into a clean, patterned Si-wafer [1,2].

In this work we present X-ray diffraction structural study of various types of Ge crystals epitaxially grown in shape of elongated pillars on prepatterned Si substrates (Fig. 1). The Ge crystals height ranged from 1 to 8 m and different patterns were explored. The typical area of pillars was ~ 2 2 m^2 separated by 1 m wide trenches.

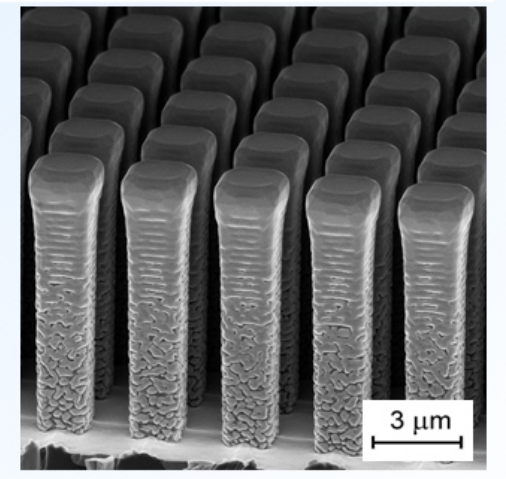

Figure 1. SEM image of epitaxial grown Ge crystals on etched 8 m Si pillars shows 1.2 m high crystals having pillar period 3 m and 1 m large trench.

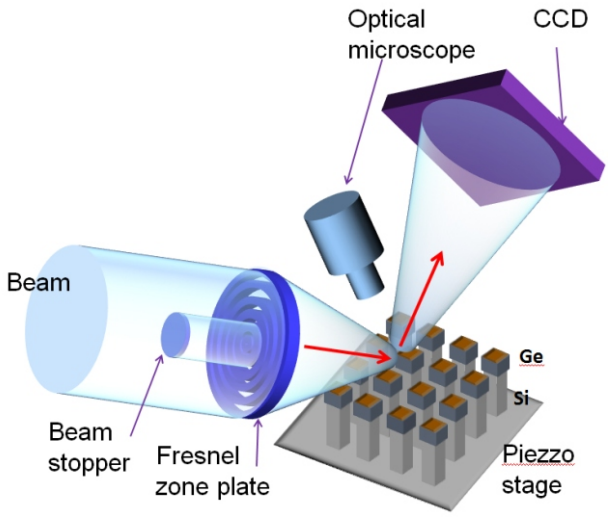

Figure 2. Experimental setup of scanning nanodiffraction experiment.

The aim of the structural investigation of the Ge pillars was to determine crystal lattice tilt and strain as from whole pillars as locally within the pillar. Thus XRD measurements in coplanar geometry around the symmetric (004), and the asymmetric (115) reflections were performed using a focused beam. The experiment was realized at ESRF, Grenoble, at the ID01 beamline, which is equipped with a Fresnel zone plate, so that the final beam spot size was ~ 500 300 nm (Fig. 2). Such condition allowed us to map the diffracted intensity across the individual pillars and to obtain (x,y) position map of diffracted intensity. Using a 2D pixel detector, 3-dimensional reciprocal space maps (RSMs) were constructed for each (x,y) position of the x-ray beam on the sample (Fig. 3).

The analysis of 3D RSMs recorded at 2D surface mesh allowed us to obtain the (x,y) map of lattice tilt, strain and relaxation within Ge pillars. The results show that the crystal planes close to Ge/Si interface are bent due to elastic relaxation of thermal strain which develops during cooling from the growth temperature. By scanning diffraction technique we were able to distinguish between lattice bending and tilts of the whole crystals. The lattice bending was in

very good agreement with the finite element calculations [3,4].

1. C.V. Falub, H. von Känel, F. Isa, R. Bergamaschini, A. Marzegalli, D. Chrastina, G. Isella, E. Müller, P. Niedermann, L. Miglio, *Science*, **335**, (2012), 1330.
2. H. von Känel and L. Miglio, international patent application WO/2011/135432.
3. C. V. Falub, T. Kreiliger, A. G. Taboada, F. Isa, D. Chrastina, G. Isella, E. Mueller, M. Meduňa, R. Bergamaschini, A. Marzegalli, E. Bonera, F. Pezzoli, L. Miglio, P. Niedermann, A. Neels, A. Pezous, R. Kaufmann, A. Dommann and H. von Känel, International Semiconductor Conference (CAS) **2**, (2012), 45.
4. C. V. Falub, M. Meduňa, D. Chrastina, F. Isa, A. Marzegalli, T. Kreiliger, A.G. Taboada, G. Isella, L. Miglio, A. Dommann, and H. von Känel, Scientific Reports **3** (2013), 2276.

We acknowledge program funding Nano-Tera through project NEXRAY, the staff of ID01beamline at ESRF, project Research4Industry (CZ.1.07/2.4.00/17.0006) and the FIRST Center for Micro- and Nanoscience of ETH Zürich for making available its infrastructure.

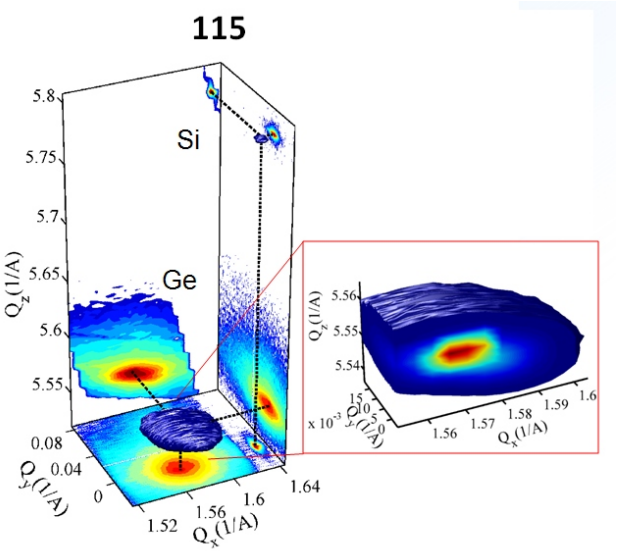

Figure 3. Example of 3D reciprocal space map recorded in the middle of the 3.1 um pillar showing detailed cut through Ge diffraction peak.

L14

CYLINDRICAL IMAGE PLATE DIFFRACTOMETER – ORIENTING AND INDEXING OF LARGE COMPACT SAMPLES IN REFLECTION MODE

Z. Matěj, J. Šmilauerová, J. Pospíšil, T. Brunátová, P. Harcuba, V. Holý, R. Kužel

Faculty of Mathematics and Physics, Charles University in Prague,
Ke Karlovu 5, 121 16 Praha 2, Czech Republic
matej@karlov.mff.cuni.cz

Introduction

Rigaku RAPID II installed in the X-ray lab at MFF UK [1] is a versatile diffractometer proposing diverse options for material analysis by X-rays. It is equipped with a three-axis goniometer and a large curved image plate (IP) detector. The instrument can be routinely utilised for single crystal structure solution as well as for powder diffraction. Residual stress or texture studies were also reported [2]. The aim of this contribution is a discussion of possibilities and limitations of this instrument, which is not as common as the Bragg-Brentano or parallel beam diffractometers. Its unique advantage, that large parts of the reciprocal space are explored simultaneously, is illustrated on an example application of the analysis of (coherent) inclusion nanoparticles in Ti-alloys.

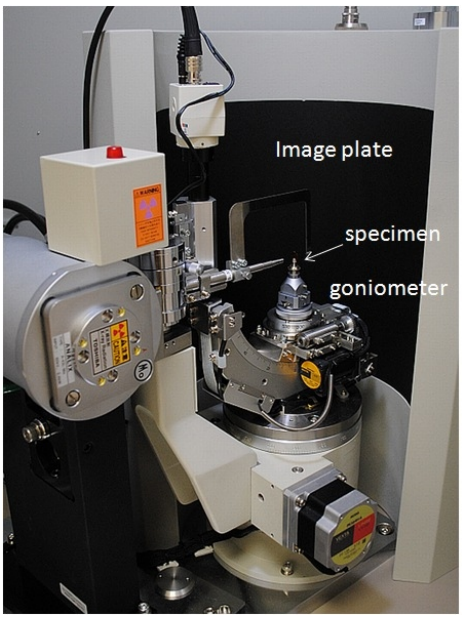

Figure 1. Rigaku R-Axis Rapid II diffractometer with image plate system.

Diffractometer, large samples and reflection geometry

The diffractometer is depicted in Fig. 1. Its standard applications include analysis of small (0.01-1 mm) single crystal samples or powders filled in glass/capton capillaries. These experiments can be done directly in transmission geometry and the advantage of the large cylindrical IP detector to capture a wide range (200°) of scattering angles is fully utilised. Contrary, for large (10 mm) compact samples of a “coin” size and thickness, which are of main interest here, the reflection geometry is the only reasonable option. A typical experiment is depicted in Fig. 2. The sam-

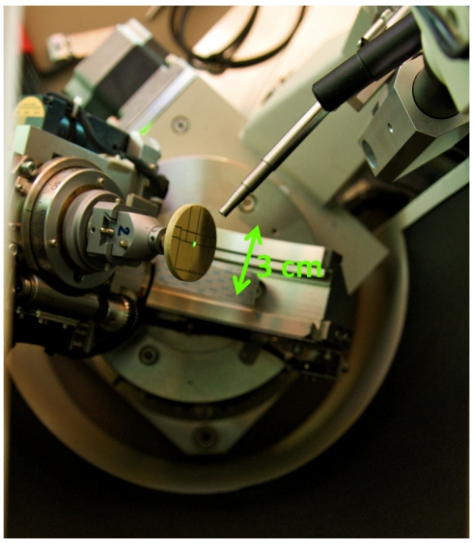

Figure 2. Florescent target mounted in the sample position. During a typical experiment two goniometer axes are set to fixed positions (*omega* = 210°, *psi* = 55°) and the sample is spinning/oscillating around the axis (*phi*) perpendicular to the sample surface.

ple surface is roughly aligned to be perpendicular to the (*phi*) spin axis. Other two goniometer axes (*omega*, *psi*) are set to general fixed positions. A quick (20-30 min) "survey" experiment can be done with sample (*phi*) spinning or a series of pictures can be acquired with crystal oscillating in small (*phi*) intervals during an "overnight" experiment.

Reference samples

In order to understand the diffraction geometry in detail and test the accuracy of the experiment the NIST standard Si powder sample and a high quality defect free Si wafer were measured under conditions described above. The analysis of the Debye rings from the powder sample is illustrated in Fig. 3. In the first step diffracted intensity at several ( ) positions on the rings was fitted with Cu-K doublet profiles. The refined experimental 2 positions were then compared with that calculated for the nominal lattice parameter and including zero-beam and sample displacement [3] corrections. This difference was smaller than ~ 0.05° on all the Debye rings. If in addition the lattice parameter was refined, the discrepancy from the nominal value was about ±0.001 Å. For single crystal data the accuracy reached was slightly worth. About 15-40 diffraction maxima were analysed. The differences in 2 positions were practically same ~ ±0.05° and the ( ) positions on the rings were predicted with ~ 0.1° error. Unfortunately the discrepancy in the lattice parameter was ±0.003Å for the single crystal experiments.

Orienting and indexing of single crystals of LCB Ti-alloy

Indexing of LCB beta-Ti alloy [4] is a challenging problem. The single crystals consist of a metastable bcc beta-Ti matrix and of a large fraction of (coherent) inclusion nanoparticles of hexagonal-Ti. The samples were analysed also by pole figures (PF) measurements and reciprocal space mapping in [5].

A preliminary analysis of the quick "survey" experiment using the Rigaku 2DP software is depicted in Fig. 4. Diffraction maxima from two different crystal systems (bcc beta-Ti matrix and inclusion of hexagonal omega-Ti phase) are simply identified. A large part of the reciprocal space is examined in this rapid experiment. This is an ad-

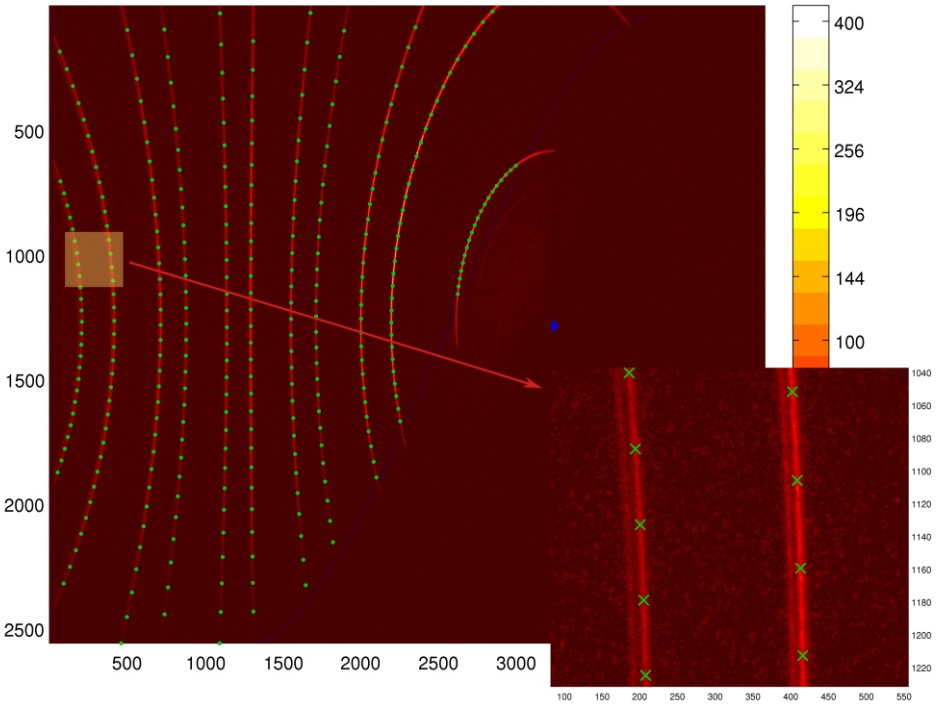

Figure 3. Analysis of Debye rings from the NIST standard Si powder sample for calibration of beam and sample displacement instrumental corrections. Diffracted intensity in the bottom right corner of the IP is shadowed by the goniometer head.

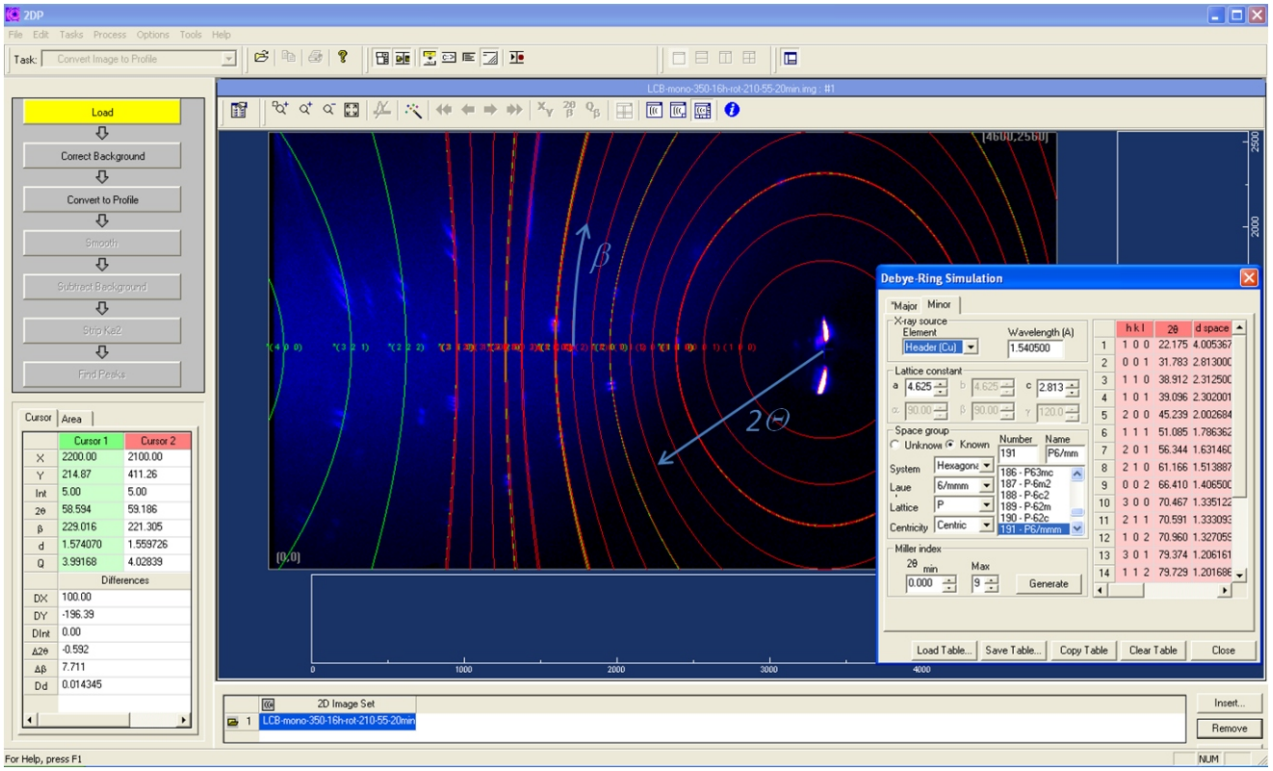

Figure 4. A preliminary analysis of the quick "survey" measurement of the LCB beta-Ti alloy single crystal using the Rigaku *2DP* software. Simulated green Debye rings are related to the (bcc) beta-Ti matrix phase. Contrary red lines come from the minor omega-Ti nanoparticles. The lattices of both phases are coherent hence some beta-Ti green rings are overlapped with red rings of (hexagonal) omega-Ti.

vantage especially if we consider that e.g. for PF measurements the line (*2Theta*) position must be known a priory. The longer "overnight" experiments brilliantly simplify the orientation and indexing procedures and enhance signal from weak diffraction maxima. An image from such a measurement is depicted in Fig. 5. Finally it was indexed by the beta-Ti matrix and four families of omega-Ti inclusions [5].

References

1. R. Kužel, *Rigaku R-Axis Rapid II at MFF UK*: www.xary.cz/kfkl-osa/eng/rapid/ (Jul 23, 2013).

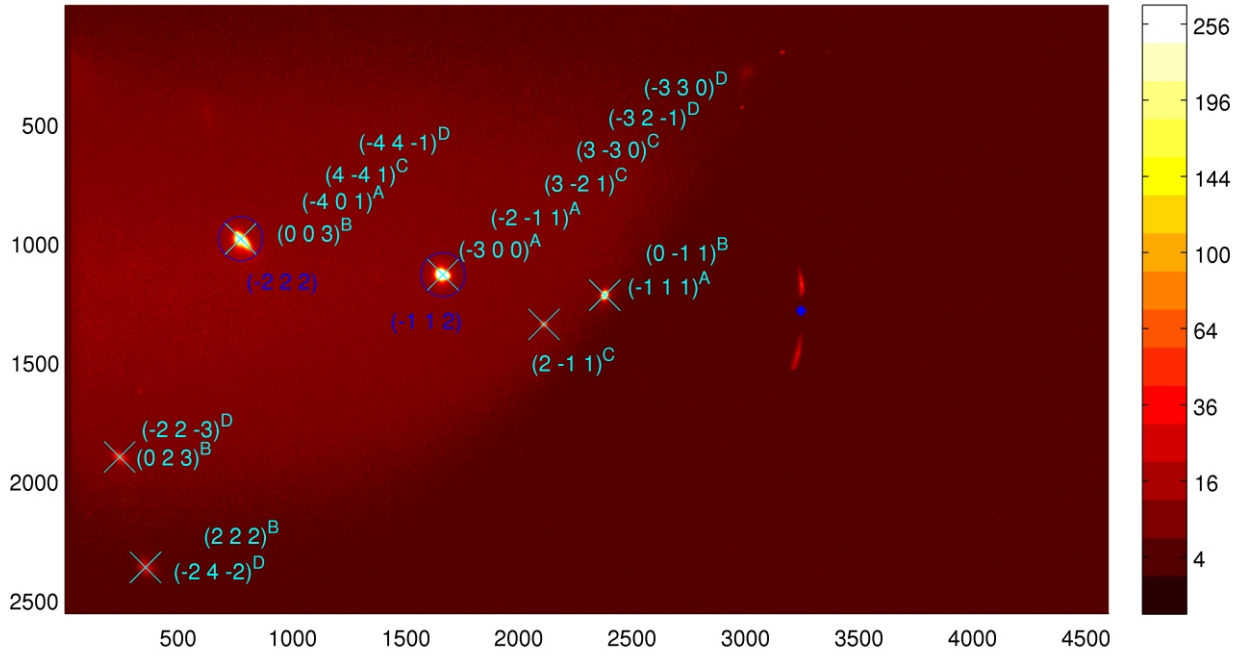

Figure 5. Possible indexing of an image taken in the oscillation mode. Intensity maxima can be indexed by (bcc) beta-Ti matrix (blue circles) and by 4 families (subindexes A, B, C, D) [5] of (hexagonal) omega-Ti (cyan crosses).

2. M. Gelfi, E. Bontempi, R. Roberti, L.E. Depero, *Acta Mat.*, **52**, (2004), 583.
3. N. V. Y. Scarlett, M. R. Rowles, K. S. Wallwork, I. C. Madsen, *J. Appl. Crystallogr.*, **44**, (2011), 60-64.
4. J. Šmilauerová, J. Pospíšil, *J. Cryst. Growth*, (2013), submitted.
5. V. Holý, J. Šmilauerová, J. Stráský, J. Pospíšil, M. Janeček, *Mat. Struct. Chem. Bio. Phys. Tech.*, **20**, (2013), a contribution in these proceedings.

This work has been supported by the Grant Agency of the Czech Republic (project no. P108/11/1539) and within the Charles University Research Center "Physics of Condensed Matter and Functional Materials" (no. UNCE 204023/2012).

L15

SAXS PORTFOLIO @ RIGAKU

Peter Oberta

Rigaku Innovative Technologies Europe, Novodvorská 994, Praha 4, CZ – 142 21, Czech Republic

Rigaku Corporation is the world largest X-ray instrument dedicated company. With more the 1400 employees worldwide, it is the world leading innovation company specified on X-ray scientific and industrial instrumentation. Covering a broad range of instrumentation from XRD, XRF, SAXS, X-ray sources (micro sources and rotating anodes) to small molecule instrumentation.

The SAXS portfolio from Rigaku contains XRD instrumentation which can be extended to SAXS experiments like the Ultima IV and the SmartLab system to specialized SAXS instrumentation like the NanoMax, NanoMax IQ and the S – MAX 3000.

In collaboration with the user community, Rigaku introduced several instrumental options unique in the SAXS market. The S – Max 3000 is the only SAXS instrument offering two sample chambers (WAXS and SAXS simultaneously), an 80 mm sample chamber offset for q – value extension (0.00464 $Å^{-1}$ – 4.85 $Å^{-1}$) and a patented 2D Kratky block for beam divergence reduction and flux adjustment. In combination with the Rigaku strongest laboratory source (FR-E rotating anode), delivering almost a bending magnet flux, the user can investigate all of sample types.

Session IV-a, Wednesday - afternoon, September 11

L16

Particle size and microstress estimation from the profiles of diffraction lines

URČOVÁNÍ VELIKOSTI KRYSTALITŮ A MIKRONAPĚTÍ Z PROFILŮ DIFRAKČNÍCH LINIÍ

M. Čerňanský

Fyzikální ústav AV ČR, v. v. i., Na Slovance 2, 182 21 Praha 8, Česká republika
cernan@fzu.cz

Většina materiálů, zejména strojírenských a stavebních, má polykrystalickou strukturu. To znamená, že se jedná o více nebo méně dokonalé malé krystaly - krystalické částice, které tvoří kompaktní těleso. Velikost a míra dokonalosti těchto částic má velký vliv na mechanické, magnetické a jiné fyzikální i technologické vlastnosti polykrystalických materiálů, které jsou důležité pro jejich výrobu a využití.

Velikost krystalických částic lze určit z profilu difrakčních linií, zejména z jejich šířky. Profil je tím užší, čím více je difraktujících rovin podobně, jako ve fyzikální optice viditelného světla je šířka spektrální linie tím užší, čím více je vrypů na mřížce, resp. čím více vrypů tvoří mřížku. Přesněji řečeno, z šířky difrakčních profilů určujeme velikost oblasti koherentního rozptylu ve směru kolmém na difraktující roviny. Obvykle je menší než velikost zrna určena metalograficky.

K naměřené šířce difrakčního profilu přispívají experimentální efekty od nenulových rozměrů zdroje primárního záření a od nenulové hloubky vnikání primárního záření do vzorku, který je rovinný a neleží tedy celý na fokusační kružnici, dále od nenulové axiální divergence, od nenulové šířky clony detektoru a od nenulové šířky spektrálního intervalu primárního záření, jakož i od nedokonalého seřízení difraktometru. Vliv těchto faktorů popisuje přístrojová funkce g, která zkresluje skutečný fyzikální profil f, který je způsoben jenom velikostí částic, mikrodeformacemi a případně dalšími fyzikálními vlivy. Měřený profil h je pak konvolucí profilů g a f. Přístrojová funkce g se obvykle zjiš uje měřením na vhodném vzorku,